Single-camera, three-dimensional particle tracking velocimetry

Kevin Peterson,[1,*] Boris Regaard,[2] Stefan Heinemann,[2] and Volker Sick[1]

[1] *The University of Michigan, Department of Mechanical Engineering, 1231 Beal Avenue, Ann Arbor, MI 48109, USA*

[2] *Fraunhofer USA, Center for Laser Technology, 46025 Port Street, Plymouth, MI 48170, USA*

[*] *petersok@umich.edu*

Abstract: This paper introduces single-camera, three-dimensional particle tracking velocimetry (SC3D-PTV), an image-based, single-camera technique for measuring 3-component, volumetric velocity fields in environments with limited optical access, in particular, optically accessible internal combustion engines. The optical components used for SC3D-PTV are similar to those used for two-camera stereoscopic-µPIV, but are adapted to project two simultaneous images onto a single image sensor. A novel PTV algorithm relying on the similarity of the particle images corresponding to a single, physical particle produces 3-component, volumetric velocity fields, rather than the 3-component, planar results obtained with stereoscopic PIV, and without the reconstruction of an instantaneous 3D particle field. The hardware and software used for SC3D-PTV are described, and experimental results are presented.

OCIS codes: (100.0100) Image processing; (110.0100) Imaging systems; (100.6890) Three-dimensional image processing; (110.4155) Multiframe image processing; (110.6880) Three-dimensional image acquisition.

References and links

1. D. L. Reuss, R. J. Adrian, C. C. Landreth, D. T. French, and T. D. Fansler, "Instantaneous planar measurements of velocity and large-scale vorticity and strain rate in an engine using particle-image velocimetry," SAE Tech. Paper, 890616 (1989).
2. R. Konrath, W. Schröder, and W. Limberg, "Holographic particle image velocimetry applied to the flow within the cylinder of a four-valve internal combustion engine," Exp. Fluids **33**, 781–793 (2002).
3. W. Choi and Y. Guezennec, "Study of the flow field development during the intake stroke in an IC engine using 2–D PIV and 3–D PTV," SAE Tech. Paper 1999–01–0957 (1999).
4. C. Brücker, "3D scanning PIV applied to an air flow in a motored engine using digital high-speed video," Meas. Sci. Technol. **8**(12), 1480–1492 (1997).
5. M. R. Bown, J. M. MacInnes, and R. W. K. Allen, "Micro-PIV simulation and measurement in complex microchannel geometries," Meas. Sci. Technol. **16**(3), 619–626 (2005).
6. M. G. Olsen and R. J. Adrian, "Out-of-focus effects on particle image visibility and correlation in microscopic particle image velocimetry," Exp. Fluids **29**(7), S166–S174 (2000).
7. R. Lindken, J. Westerweel, and B. Wieneke, "Stereoscopic micro particle image velocimetry," Exp. Fluids **41**(2), 161–171 (2006).
8. M. P. Arroyo and C. A. Greated, "Stereoscopic particle image velocimetry," Meas. Sci. Technol. **2**(12), 1181–1186 (1991).
9. M. R. Bown, J. M. MacInnes, R. W. K. Allen, and W. B. J. Zimmerman, "Three-dimensional, three-component velocity measurements using stereoscopic micro-PIV and PTV," Meas. Sci. Technol. **17**(8), 2175–2185 (2006).
10. R. Lindken, J. V. Esch, J. Westerweel, and B. Wieneke, "3D particle imaging for the quantitative characterization of advective microscale mixing," in 14th Int. Symp. on Applications of Laser Techniques to Fluid Mechanics (2008).
11. X. Bao and M. Li, "Defocus and binocular vision based stereo particle pairing method for 3D particle tracking velocimetry," Opt. Lasers Eng. **49**(5), 623–631 (2011).
12. B. Wieneke, "Volume self-calibration for 3D particle image velocimetry," Exp. Fluids **45**(4), 549–556 (2008).
13. G. E. Elsinga, F. Scarano, B. Wieneke, and B. W. Oudheusden, "Tomographic particle image velocimetry," Exp. Fluids **41**(6), 933–947 (2006).
14. K. Ohmi and H. Y. Li, "Particle-tracking velocimetry with new algorithms," Meas. Sci. Technol. **11**(6), 603–616 (2000).

#162385 - $15.00 USD Received 1 Feb 2012; revised 12 Mar 2012; accepted 28 Mar 2012; published 3 Apr 2012

15. M. Ishikawa, Y. Murai, and F. Yamamoto, "Numerical validation of velocity gradient tensor particle tracking velocimetry for highly deformed flow fields," Meas. Sci. Technol. **11**(6), 677–684 (2000).
16. R. D. Keane, R. J. Adrian, and Y. Zhang, "Super-resolution particle imaging velocimetry," Meas. Sci. Technol. **6**(6), 754–768 (1995).
17. H. S. Tapia, J. A. G. Aragón, D. M. Hernandez, and B. B. Garcia, "Particle tracking velocimetry (PTV) algorithm for non-uniform and non-spherical particles," Electronics, Robotics and Automotive Mechanics Conference, **2**, 325–330, (2006).
18. A. V. Mikheev and V. M. Zubtsov, "Enhanced particle-tracking velocimetry (EPTV) with a combined two-component pair-matching algorithm," Meas. Sci. Technol. **19**(8), 085401 (2008).
19. N. J. Lawson and J. Wu, "Three-dimensional particle image velocimetry: error analysis of stereoscopic techniques," Meas. Sci. Technol. **8**(8), 894–900 (1997).
20. C. E. Willert and M. Gharib, "Digital particle image velocimetry," Exp. Fluids **10**(4), 181–193 (1991).

1. Motivation

The performance of internal combustion engines is strongly dependent on the in-cylinder air flow, thus experimentally characterizing engine air flow is critical to optimizing engine performance. Engine flows have been studied using a variety of techniques, including planar PIV [1], holographic PIV [2], 3D PTV [3], and scanning PIV [4]. However, these techniques are not well suited to studying all important aspects of engine flows, such as boundary layer flows or flows near the engine head while the piston is at the top of its travel. The primary obstacles to studying these flows are: 1) a highly 3D nature with characteristic structures on a millimeter length scale 2) structures that evolve on a millisecond time scale 3) limited optical access.

Single-camera, 3D particle tracking velocimetry (SC3D-PTV) has been developed to address these obstacles. SC3D-PTV is designed to use a single camera to measure three-component, volumetric velocity fields over a limited measurement volume at high spatial and temporal resolution with only two points of optical access.

2. Experimental set-up

The optical arrangement of SC3D-PTV is closely related to stereoscopic-μPIV [5], which uses coaxial illumination and two off-center optical paths through a single lens to create two imaging sub-systems with different viewing angles. SC3D-PTV also employs one main lens and two off-center apertures, with two smaller lenses in the apertures. Instead of coaxial illumination, which causes noise from out-of-plane particles [6], volume illumination propagating in the object plane of the imaging system is used for SC3D-PTV.

Unlike traditional two-camera stereoscopic arrangements that use Scheimpflug adapters, the optical arrangement of SC3D-PTV creates two views of the same measurement volume without perspective distortion. Two simultaneously acquired images are focused to a single camera using a "beam twister" mirror setup. This mirror arrangement re-orients the images by 90° to use the image sensor space most efficiently. A schematic of the optical arrangement is seen in Fig. 1.

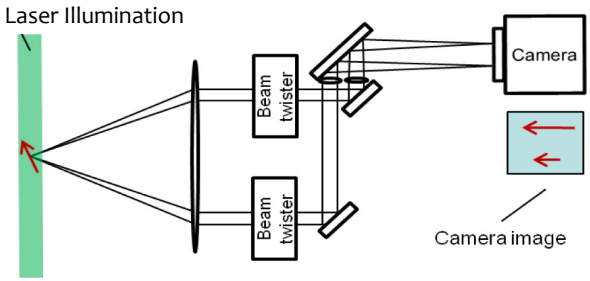

Fig. 1. Two off-center optical paths through a single lens create two views of the measurement volume. A mirror arrangement rotates the images by 90° to use the space of a single image sensor most efficiently.

All imaging optics are packaged in a sealed housing (approximately 15cm x 15cm x 20cm) that mounts directly to the camera in order to reduce alignment complexity, protect the optics from contamination, and minimize the experimental footprint of SC3D-PTV. An addi-

#162385 - $15.00 USD Received 1 Feb 2012; revised 12 Mar 2012; accepted 28 Mar 2012; published 3 Apr 2012

tional image cropping optic with an internal aperture (not shown, approximately 30cm x 5cm dia.) can also be used to eliminate cross-talk between the two imaging sub-systems.

3. Image analysis

For frame-straddling stereoscopic-µPIV measurements, as in SC3D-PTV analysis, a total of four images are processed to obtain a single vector field. Two image pairs are captured successively, and an image pair consists of one image from each of the two viewing angles. Early papers describing stereoscopic-µPIV [5,7] use stereoscopic-PIV algorithms based on cross-correlation [8] to obtain three-component two-dimensional (3C2D) results. Later papers [9–11] show the use of particle tracking algorithms to obtain 3C3D results from the same 4-image data sets. Particle tracking algorithms require two critical processing steps: the matching of simultaneously acquired particle images to determine the instantaneous 3D positions of the tracer particles (simultaneous matching), and the matching of successively acquired particle images to determine particle displacement (successive matching).

The two matching processes provide sufficient information to reconstruct the 3D particle displacement and locate the vector in 3D real space. These matching processes can be performed in 2D image space, eliminating the need to reconstruct a voxel space or an instantaneous 3D particle field prior to computing the 3C3D vector field.

Several approaches for finding simultaneous matches are found in the literature. Lindken et al. [10] use the volume self-calibration method proposed by Wieneke [12], in which a particle at a given image location in one view can only be matched to a subset of the possible image locations in a different view, using epi-polar line considerations. When using two views, a method based on intersecting epi-polar lines can only tolerate low seed densities without ambiguity [13].

Bao and Li [11] also use the method of intersecting epi-polar lines to find simultaneous image matches, but the degree-of-defocus of the particle image provides an additional constraint to the algorithm, allowing higher seed densities than an algorithm relying solely on epi-polar lines. The simultaneous matching performed during SC3D-PTV analysis is based on the concept of epi-polar lines with additional image-similarity constraints.

Numerous methods also exist for determining successive particle images corresponding to the same particle. Some methods rely on the similar motion of groups of particles that are spatially-clustered in image space, such as the relaxation method [14], the minimization of the velocity gradient [15], or cross-correlation-based super-resolution PIV [16]. For measurement volumes with a depth on the order of the size of the characteristic vortices of the flow these methods cannot be applied, because a particle near the front of the measurement volume and a particle near the back of the measurement volume could be projected onto the same area in image space, but be travelling in opposite directions.

Tapia et al. [17] use an extended nearest-neighbors method which examines all particle images within a defined radius and uses the intensity and shape of individual particle images as additional matching criteria. Similarly, Mikheev and Zubtsov [18] add size-similarity and intensity-similarity thresholds to a nearest-neighbors algorithm. It is the notion of a nearest neighbors search supplemented with additional particle image-similarity criteria that is the basis of SC3D-PTV successive matching.

For SC3D-PTV analysis, initially the raw images are analyzed using a two-stage threshold to find particle images. Epi-polar line considerations are used to define possible simultaneous matches. Possible successive matches are those within a radius determined by maximum estimated flow velocity. Then, all possible simultaneous and successive matches are examined to find ‘complete 4-image sets.’ A complete 4-image set is a group of two different simultaneous matches and two different successive matches that contains only four total particle images.

It is likely that each particle image will be included in more than one complete 4-image set, but in the absence of overlapping particle images, each particle image can be included in only one valid complete 4-image set, i.e. a complete 4-image set that leads to a valid vector. If multiple 4-image sets contain the same particle image, only the 4-image set whose matches

#162385 - $15.00 USD Received 1 Feb 2012; revised 12 Mar 2012; accepted 28 Mar 2012; published 3 Apr 2012

display the highest degree of similarity is chosen as a valid 4-image set. Particle image similarity is defined using seven criteria: 1) peak intensity 2) summed intensity 3) total number of pixels 4) width, as measured in pixels 5) height, as measured in pixels 6) maximum value of a cross-correlation between zero-padded raw particle images 7) maximum value of a normalized cross-correlation between zero-padded binarized particle images.

The appropriate similarity threshold for each feature was determined experimentally. A series of sparsely-seeded data were acquired from an air jet seeded with silicon oil droplets (~1 μm diameter) over a measurement volume of 6mm x 6mm x 2mm (and further details of the experimental configuration can be found in the Section 4). The sparsely-seeded data were used to provide complete 4-image sets that could be unambiguously verified using position assumptions alone, without using particle image similarity considerations. Because the images were sparsely seeded, most particle images were members of only a single 4-image set. All 4-image sets whose members were not part of any other 4-image set were considered valid regardless of the similarity of the particle images. A control group of invalid matches was formed by randomly matching particle images from non-consecutive raw images, such that the particle images were guaranteed to correspond to different particles because the same particles were not present in all raw images. 8,000 likely-valid matches and 10,000 invalid matches were analyzed, and no single feature was found to fully separate valid and invalid matches. As an example, Fig. 2 shows the cumulative density function of the width difference for the valid matches and the invalid matches. At a threshold level where 90% of the valid matches are retained, approximately 30% of the invalid matches are also retained. It is likely that the threshold values will change for different experimental conditions, but the new threshold values can be quickly calculated from a sparsely-seeded data set taken under each set of conditions.

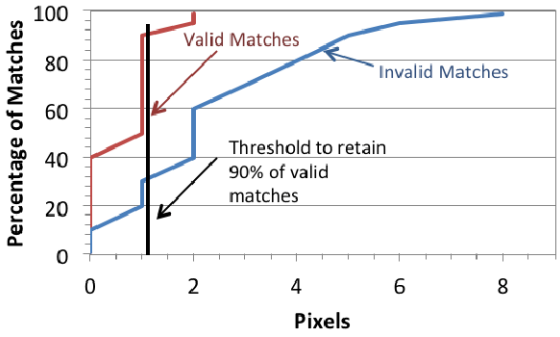

Fig. 2. The cumulative density function of the width difference of valid and invalid matches shows that at a threshold where 90% of the valid matches are retained, 30% of the invalid matches are also retained.

Although no single feature separates the valid and invalid 4-image sets, by setting a threshold on all seven features, and comparing each simultaneous and successive match within a 4-image set (28 total comparisons), the valid and invalid 4-image sets can be largely separated. The threshold is set at the level where 90% of the valid matches are retained. As seen in Fig. 3, 36% of valid sets, but only 1% of invalid sets, exceed the 90% threshold on all 28 compared features. After separating valid and invalid sets using feature comparisons, calibration data from the imaging of a calibration plate imaged at known depths is used to determine the 3D particle displacement and 3D vector position in real space for all valid sets.

#162385 - $15.00 USD Received 1 Feb 2012; revised 12 Mar 2012; accepted 28 Mar 2012; published 3 Apr 2012

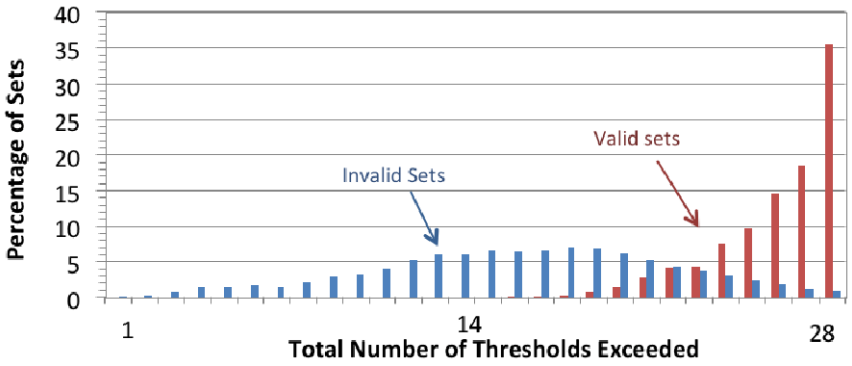

Fig. 3. A threshold value for each feature is set at the level where 90% of the valid matches are retained. Valid sets are much more likely than invalid sets to exceed the 90% threshold for every feature comparison, allowing valid and invalid sets to be separated using feature comparisons.

4. Proof of principle

Validation of the SC3D-PTV technique was achieved through analyzing a single experimental data set collected with the SC3D-PTV optic using both the SC3D-PTV algorithm and a stereoscopic PIV algorithm. For the stereoscopic PIV (SPIV) results, the DaVis commercial flow analysis software package from LaVision GmbH was used to compute 2C2D PIV flow fields separately for each viewing angle, and the 3C2D flow fields were reconstructed using knowledge of the relative angle of the two viewing angles.

The flow under study was the air exiting from a 12.5 mm inner diameter hose into ambient conditions. The air was seeded with silicon oil droplets (diameter: 1 micron) using a TSI 9306 atomizer. Pairs of temporally-separated images were collected at 1 kilohertz using a Phantom camera (Vision Research, v7.3), the SC3D-PTV optic, and one-to-one image cropping optic. Image pairs were separated by 20 microseconds using a frame-straddling approach. Illumination was provided by a Quantronix Darwin Duo laser operating at 527 nanometers and gave 500 micro-joules of energy per pulse over a measurement volume of 6x6x2 millimeters (2 millimeters in the out-of-plane direction). The measurement volume was defined by the thickness of the laser sheet and the size of the aperture inside the image cropping optic. The experimental set-up is shown in Fig. 4.

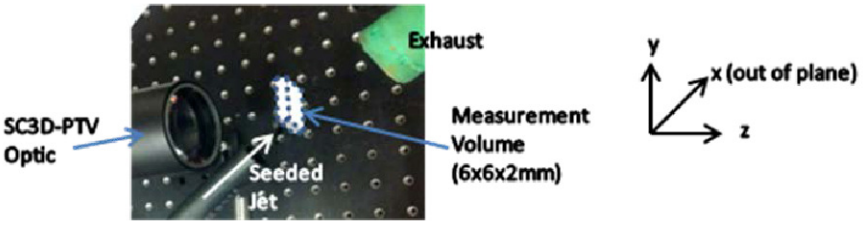

Fig. 4. Experimental set-up. An air jet seeded with silicon oil droplets was studied by illuminating the droplets with laser light and imaging the flow using the SC3D-PTV optic attached to a high-speed camera.

The vectors computed using the SC3D-PTV algorithm were randomly located within the measurement volume. To facilitate both averaging of SC3D-PTV velocity fields and comparison of the SPIV and SC3D-PTV results, the randomly-located SC3D-PTV vectors were linearly interpolated onto a single-plane grid of the same spacing as the SPIV results (32x32 pixels). 100 SC3D-PTV measurements taken over a 100 millisecond time interval were averaged, and the result is shown on the left in Fig. 5. The right image in is computed from the

#162385 - $15.00 USD Received 1 Feb 2012; revised 12 Mar 2012; accepted 28 Mar 2012; published 3 Apr 2012

same data as the left image, but shows the average of 100 instantaneous vector fields calculated using the SPIV algorithm.

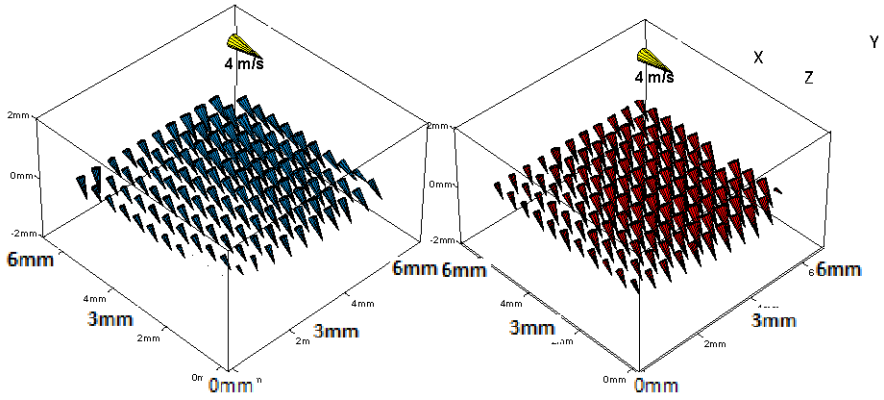

Fig. 5. (Left) Using the SC3D-PTV algorithm, an average velocity field was calculated from 100 instantaneous flow measurements taken over an interval of 100 milliseconds. (Right) The same raw data was used to compute 100 SPIV velocity fields, and the average velocity field was computed.

At a qualitative level, both algorithms produce very similar results, although some disagreement is seen near the edges of the measurement volume, where both techniques suffer from particles entering and leaving the measurement volume between exposures. The comparison can be made quantitative by looking at the velocity profiles shown in Fig. 6. The two profiles are qualitatively similar, and agree closely quantitatively. The average velocity difference between the two results is 3% and the maximum difference at a single point is 9%. Using sub-pixel interpolation, the in-plane velocity component of SPIV can be measured with an uncertainty of about 0.1 pixels [19]. For SPIV, the uncertainty in the out-of-plane component is largely determined by the angle between the two views, with the uncertainty at a minimum at an angular separation of 90°. For an angular separation of about 20°, as in the SC3D-PTV optic, the uncertainty in the out-of-plane component is about five times larger than the uncertainty of the in-plane component, or 0.5 pixels [20], thus the SC3D-PTV and SPIV results agree within the uncertainty of SPIV.

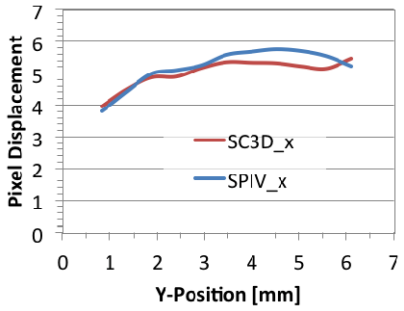

Fig. 6. The velocity field is integrated along the x-axis for both the SC3D-PTV results and the SPIV results, and the profiles are compared. The general shapes of the profiles agree, the average velocity difference is 3% and the maximum difference is 9%.

5. Engine results

Engine flow measurements were performed in a single-cylinder direct-injection optical engine. The measurement volume was located between the intake and exhaust valves, near the edge of the piston bowl.

#162385 - $15.00 USD Received 1 Feb 2012; revised 12 Mar 2012; accepted 28 Mar 2012; published 3 Apr 2012

The experiments were performed at 600 RPM. Intake manifold pressure was 95 kPa, with oil and water at 50° C and the intake air at 25° C. The intake air flow was seeded with silicon oil droplets (nominal diameter: 1 μm) using an atomizer (TSI model 9306). The atomizer pressure (~7-35 kPa) was adjusted to produce a seed density between 1 and 10 particles per cubic millimeter. The droplets were illuminated using a Quantronix Dual-Hawk II, frequency-doubled Nd:YAG laser operating at 532 nm. Each of the two laser heads operated at 1.8 kHz, producing approximately 10 W of average power each. Image pairs were captured at 1.8 kHz.

To represent the type of flow fields that can be measured using SC3D-PTV, a single instantaneous vector field computed from a single image pair taken inside the engine, and interpolated onto two planes, is shown in Fig. 7. Because SC3D-PTV measures all three components of the flow over a volume, instantaneous volumetric vortex structures like the one seen below can be characterized.

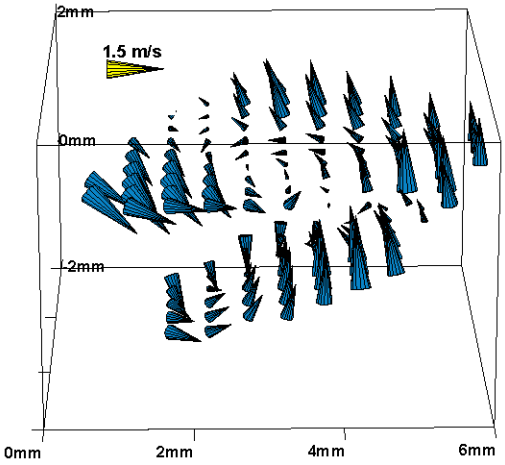

Fig. 7. An instantaneous vector field computed from data taken inside an optical engine shows a volumetric vortex structure.

6. Conclusions

SC3D-PTV is an image-based, single camera flow measurement technique capable of acquiring 3-component velocity fields over a volume. The optical components used for this technique are similar to those used for stereoscopic-μPIV, but additional mirrors are used to project two simultaneous images onto a single image sensor and orient the images to use the sensor space most efficiently. The analysis of the images relies on the similarity of the particle images corresponding to a single, physical particle and produces 3-component, volumetric velocity fields without the reconstruction of an instantaneous 3-dimensional particle field. Proof-of-principle tests were performed on a simple flow, and the same experimental data set was analyzed with both the SC3D-PTV algorithm and a stereoscopic PIV algorithm. Experimental results taken inside a motored, optically accessible combustion engine are also shown and demonstrate the ability of SC3D-PTV to capture complex volumetric flow structures.

Acknowledgments

This work was supported through the University of Michigan-Fraunhofer Alternative Energy Technologies for Transportation program and The University of Michigan-General Motors Collaborative Research Laboratory on Engine Systems Research.

#162385 - $15.00 USD Received 1 Feb 2012; revised 12 Mar 2012; accepted 28 Mar 2012; published 3 Apr 2012